

Article

# Real-time hardware-in-loop system based validation of vehicle-grid interface for bidirectional power flow control

P. N. Kapil<sup>1,2</sup> and Amit V. Sant<sup>1,\*</sup>

<sup>1</sup> Department of Electrical Engineering, Pandit Deendayal Energy University, Gandhinagar, Gujarat, India

<sup>2</sup> Department of Electrical Engineering, Nirma University, Ahmedabad, Gujarat, India

\* Correspondence: amit.sant@sot.pdu.ac.in

Received: 13 October 2023; Accepted: 15 May 2024; Published: 22 June 2024

**Abstract:** In the context of modern sustainable transportation technology, the terms Vehicle-to-Grid (V2G) and Grid-to-Vehicle (G2V) holds significant value. During V2G and G2V modes, vehicle and grid exchange power using various power converters to modulate the power for a sustainable electrical energy ecosystem. With V2G, the EVs can also perform the role of a peak power contributor, reserve power source, and an efficient system to improve power quality issues by working as power factor corrector, reactive power compensator, and active power filter, to name a few during the V2G mode. The on-board power converter in the vehicle, working as the charger for the battery, is the component required to facilitate the intended bidirectional power exchange between the vehicle and grid and also modulates the power as and when required. The modality for operating the onboard charger as a power exchange tool depends on the type of control strategy adopted as well as on the battery and grid parameters. In this paper, a bidirectional power converter (on-board converter) is introduced, which is controlled by adopting a d-q axis-based control strategy. The MATLAB/SIMULINK-based system simulation model is created, and the Hardware-in-Loop (HIL) tool Opal-RT 4510 is used to validate the simulation results on the intended hardware and real-time scenario. The control strategy, when integrated with the adopted model, contributes to enhancing the power-transferring capability of the converter, which is assessed using the simulation and subsequent HIL-based implementation. The paper also focuses on narrating the steps to implement the vehicle-grid interface using HIL and forming a generic reference model for a bidirectional power flow converter, such that it can be used for other circuits and its implementation in real-time scenarios.

© 2024 by the authors. Published by Universidad Tecnológica de Bolívar under the terms of the [Creative Commons Attribution 4.0 License](https://creativecommons.org/licenses/by/4.0/). Further distribution of this work must maintain attribution to the author(s) and the published article's title, journal citation, and DOI. <https://doi.org/10.32397/tesea.vol5.n1.567>

**How to cite this article:** Kapil, P. N.; Sant, Amit V.. Real-time hardware-in-loop system based validation of vehicle-grid interface for bidirectional power flow control. *Transactions on Energy Systems and Engineering Applications*, 5(1): 567, 2024. DOI:10.32397/tesea.vol5.n1.567

## 1. Introduction

Since the turn of the new century, electric vehicles (EVs) have become synonymous with sustainable transportation. The new order for the adoption of any technology has undergone a paradigm shift with the global focus on greener, cleaner, and sustainable technologies with minimum carbon footprint. EVs match this criteria and provide a more efficient, cleaner, and high-performance technology based alternative. Larger on-road adaptation of EVs necessitate frequent charging requirements, which would impose a great burden on electric grid. Solar photovoltaic energy can be one of the solution for meeting the increased energy demand. Alternately, EVs can also be considered as a potential source of electrical power and can be used to charge another EV. However, this would necessitate grid connection of both the EVs. An EV would transfer the power stored in its battery to the grid, while the other EV would charge drawing the power from the grid. This has given birth to the concepts of Grid-to-Vehicle (G2V) and Vehicle-to-Grid (V2G) interface [1–4]. The intent and requirement of the vehicle-grid interface is inspired by the sustainable energy-based endeavors that have been mandated on various national and international forums for quite some time to overcome the ever-increasing energy demand.

In the V2G concept, the EVs act as a power source and supply it to the power grid; conversely, in the G2V concept, the grid acts as a power source and transfers the said power to the battery for charging it [5]. V2G concept, apart from acting as a potent standalone power source, can also work as a grid-tied source if the battery has sufficient energy [5, 6]. The V2G mode also supports by acting as a reactive power compensator at the point of common coupling with the grid. In addition to this, the V2G can also help in acting as a shunt-connected power stability device and also as a peak-shaving power source for the grid during the time of higher demand on the grid [5]. The grid can benefit from the auxiliary services that V2G-capable EVs can offer, like frequency regulation, voltage support, and grid stability [7, 8].

Since the turn of last decade, the EV penetration and its adoption has increased manifold. This meteoric rise of EVs has led to drastic implications for the power sector. The presently available generation and installed capacity is not able to match up with the increment in the demand led by EVs. This disparity has started to put lot of stress on the power grid. To relieve the grid from this power crunch, EVs can be used as a potent option to support bridging the power gap. V2G mode employs the capability of EV to transfer power from the battery to the power grid [9–11]. However, V2G mode is not just limited to infusing active power into the grid from the battery, but also meets fully or partially the reactive power demand of the system at the point of common coupling [12].

V2G talks about utilizing the energy stored in the EV battery, whereas on the other hand G2V talks about supplying the energy for the battery charging. Frequent movement of an EV results in depletion of charge stored in the battery. Hence, G2V operation, which deals with transfer of power from grid to EV for charging the EV battery, is essentially required. For G2V, the battery pack is interfaced with the grid through an on-board or off-board converter [1, 2]. However, for this, EVs need to be connected to the grid and they should be in a position to receive electric power. Hence, charging points or charging station with different charging points are needed for G2V operation [13]. Depending on the infrastructure for charging and the EV's battery capacity, G2V charging can proceed at various rates [14].

The broader idea of smart grids and energy management includes both V2G and G2V technologies. By utilizing the ability of EV batteries to store and supply electricity, they contribute to a more dynamic and flexible energy system. These ideas could be very important for improving grid stability, incorporating renewable energy sources, and reducing energy use [5, 6, 8]. However, in order for them to be widely adopted, there are a number of technical, financial, and legal issues that must be resolved. These issues include issues with battery deterioration, communication protocols, and regulatory frameworks that promote participation from both EV owners and grid operators [13].

The paper presents the concept of V2G and G2V energy transfer using the inverter and  $dc - dc$  converters integrated with closed-loop control. The intent behind the work is to present a methodology using a fast prototyping-based system using HIL. The work presented here is to highlight and showcase a methodical way of implementing a vehicle-grid interface converter using HIL to be used as a reference for modeling other intricate systems for research purpose. In this work, investigation on V2G and G2V interface modes employing an  $ac - dc$  and bidirectional  $dc - dc$  converter along with their individual control strategies is employed in both simulation as well as HIL environment. The results for various operating modes in steady state and dynamic condition is discussed in detail with their results.

The key highlights of the paper are:

1. Creating and executing a control scheme on MATLAB/SIMULINK to demonstrate a seamless transfer of power between the vehicle and the grid simultaneously, assuring that the power quality at the grid side is maintained in accordance with the widely recognized standards.
2. A thorough understanding of the HIL system and the application of the model created in MATLAB/SIMULINK on the HIL, which reduces the amount of time needed to construct and test a hardware circuit.
3. Verifying the execution of the bi-directional power flow between the grid and the vehicle by validating and contrasting the simulation study results with the HIL findings.

## 2. Vehicle grid interface mode

### 2.1. G2V operation

G2V operation is critical for EVs. EVs utilize the energy stored in the battery pack for developing the necessary tractive effort [9–11]. Hence, the EV batteries need to be frequently charged from the grid. G2V operation facilitates the charging of the battery pack. As batteries require dc power whereas the grid supplies ac power, power converter facilitating  $ac - dc$  conversion is required. Pulse width modulated (PWM) rectifiers can facilitate  $ac - dc$  conversion while ensuring that the currents drawn from the grid are sinusoidal and in-phase with the corresponding grid voltages measured at the point of common coupling. With PWM boost rectifiers, the magnitude of output dc voltage is higher than the peak value of ac grid voltages. However, the battery voltage is more often than not lower than the output dc voltage of the PWM boost rectifier.

The battery needs to be charged in constant current charging mode, constant voltage charging mode, or pulse charging mode. The level of charging and rate of charging depends upon the present state of charge

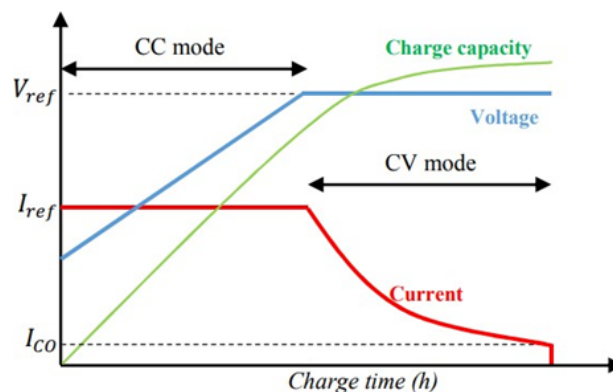


Figure 1. Charging profile of battery.

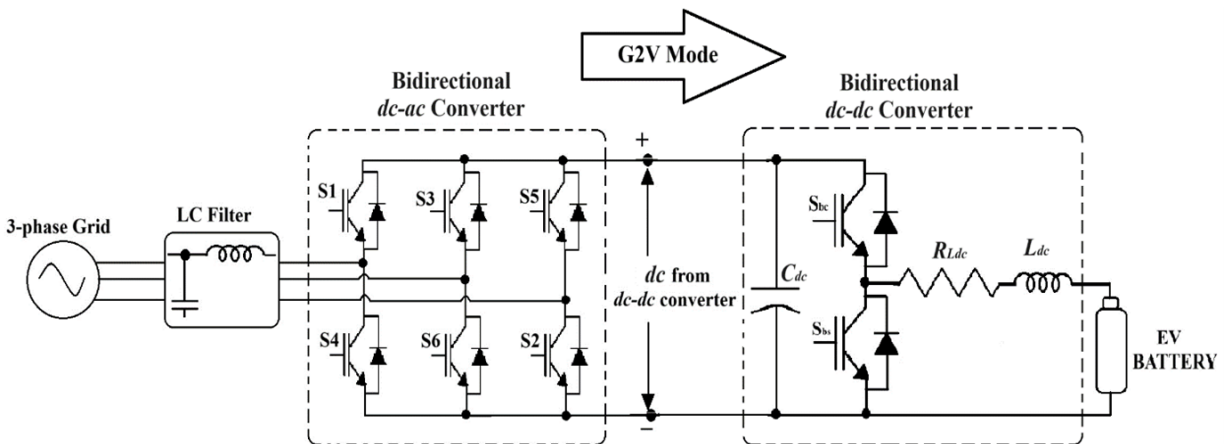


Figure 2. G2V operation block diagram.

of the battery, which in turn decides the type of charging methods like constant current or constant voltage charging mode. The battery charging at a lower state of charge is primarily done using the constant current method, and once the battery voltage reaches a cut-off voltage set by the charger, the charging method switches over to the constant voltage method [15]. The correlation of the various parameters like voltage, current, charge, and time is shown in Figure 1, where  $V_{ref}$  is the maximum permissible voltage across the battery pack,  $I_{ref}$  is the maximum permissible charging current that can be supplied to the battery pack and  $I_{co}$  is the minimum cut-off current corresponding to the fully charged condition of the battery pack at which the charging stops [16]. Moreover, certain precautions must be taken to ensure the safe operation of the battery pack. This includes continuous monitoring of various parameters of the battery, like voltage, current, temperature, and state of charge, to prevent overcharging and deep discharge of the battery pack. This can lead to a seamless transition of the charging mode from one to the other. Charging of the battery as per the selected mode can be achieved with the incorporation of a  $dc - dc$  converter between the PWM rectifier and the battery.

The power circuit for G2V operation is pictorially represented in Figure 2. In this mode involves battery charging with the power flowing from grid to the battery. For the constant voltage charging, the  $dc - dc$  converter can control the output dc voltage as per the battery requirement. Conversely, for constant current charging mode, the  $dc - dc$  converter can control the output current as per the commanded C-rate at which the battery needs to be charged. However, it must be noted that with boost PWM rectifier the dc-link voltage is higher than the peak value of the line-line grid voltages. Hence, the  $dc - dc$  converter needs to step down the voltage as per the battery requirement. In addition to  $ac - dc$  conversion, the PWM rectifier regulates the  $dc$ -link voltage at the commanded value and ensures that sinusoidal current are drawn from the grid at unity power factor.

## 2.2. V2G operation

V2G is a relatively new feature for EVs that allows the user to be a prosumer. This operation would be specifically useful for peak shaving, reactive power compensation, harmonic current mitigation. It can support the grid by contributing active and reactive power as per the requirement. With the battery being a dc source whereas the grid being an ac source, for V2G mode of operation an inverter is essentially required. Moreover, for grid synchronization of any distributed energy resource (DER), such as a battery, it is essential that the phase, frequency, and voltage of the DER should match with that of the grid. Hence, the inverter employed as a basic building block in the V2G operation performs the power modulation action

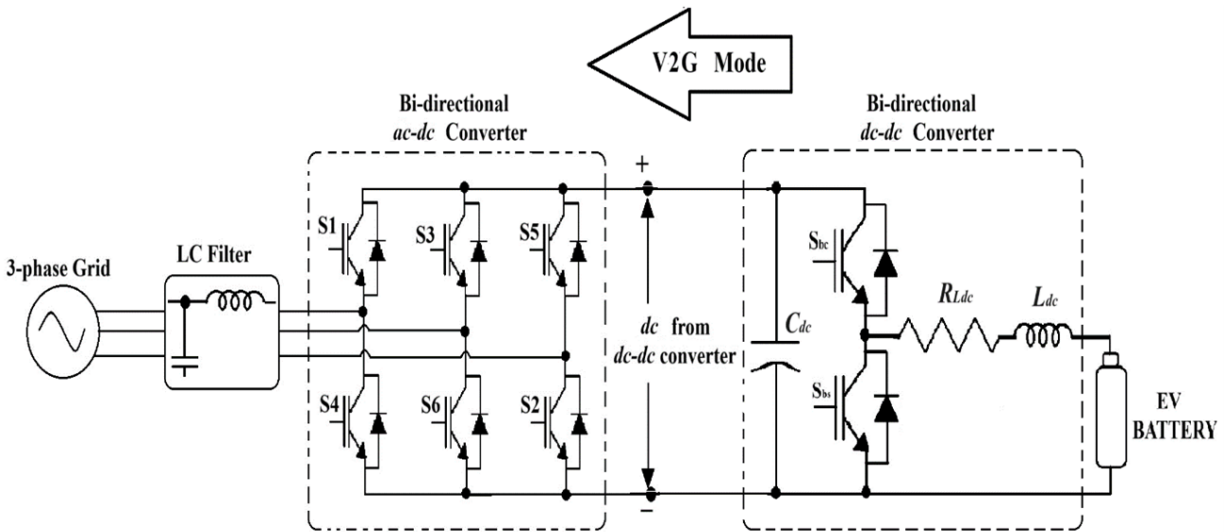


Figure 3. V2G operation block diagram.

by matching the phase and frequency of the output voltage with that of the grid. For matching voltages, the  $dc$ -link voltage needs to be controlled. Normally considering a fully charged battery, the terminal voltage is lower compared to the peak value of the three-phase grid voltage. Hence, the battery voltage needs to be stepped up. Additionally, the discharging of the battery pack needs to be controlled so that the recommended C-rate limit is not breached. These two requirements can be met with a  $dc - dc$  converter. Hence, in V2G mode of operation, the  $dc - dc$  converter is used as an interface between the inverter and the battery [17]. The pictorial description of the V2G operation is shown in Figure 3.

The synchronization of inverter output voltage at the grid interface is carried out using phase-locked loop (PLL). There are various methods employed for the implementation of the grid-tied system using PLL [18] and the method employed and discussed briefly here is synchronous reference frame (SRF) based PLL. The SRF PLL consists of three stages or building blocks viz. phase detector (PD), loop filter (LF) and a voltage-controlled oscillator (VCO). In SRF-PLL, the 3-phase grid voltages undergo abc-to-dq transformation. Initially, the phase angle is assumed to be zero. The resulting q-axis voltage should be zero as the grid voltage would not have any quadrature component. However, as the phase angle has been assumed, this may not be the case. Hence, the q-axis voltage is compared with the reference value of

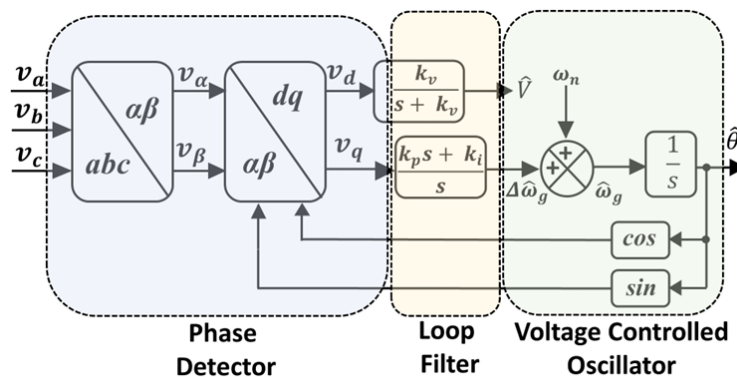


Figure 4. SRF PLL block diagram.

zero, and the resulting error is processed by the PI controller to determine the grid frequency. The grid frequency is integrated with respect to time for determining the phase angle, which is utilized at the next sampling instant for carrying out  $abc - to - dq$  transformation. When the correct value of the phase angle is determined, the quadrature voltage becomes zero, and consequently, the output of PI controller (i.e. grid frequency) is held constant as a result of the previous output of integral action. It is to be noted that the estimated frequency matches the grid frequency. The implementation block diagram of PLL used in the paper can be understood by referring to Figure 4.

### 2.3. Mode transitions

The V2G mode of power transfer requires  $dc - dc$  converter to be able to extract the dc power from the battery and progressively supply it to the PWM inverter to be able to convert dc to ac and then supply ac power into the grid. The PWM inverter in this case acts as a grid tied inverter, enabling seamless power transfer from EV to the three-phase grid. The nature of power injected into the electrical grid from the battery pack is active power. Conversely, in the G2V mode, the power flow, as expected, reverses. This mode corresponds to the charging of the EV battery pack from the three-phase grid. The power flows from the grid into the PWM inverter, which, without any change in the power structure, now acts as a PWM rectifier. The said PWM rectifier converts the ac into dc with a certain order of boost in it which then is supplied to the battery pack. Since the dc voltage available is a higher than the permissible dc voltage of the battery which can be harmful if supplied to the battery pack. To avoid this situation, the  $dc - dc$  converter stage already available as an interface between PWM inverter and battery pack will come into play and will reduce the dc voltage to the level desirable at the terminals of the battery deemed suitable for charging it. This unique requirement of the G2V mode necessitates the  $dc - dc$  converter stage to be bi-directional in nature. The  $dc - dc$  converter stage in such situations is different from the conventional converters as they are bi-directional on account of their power structure.

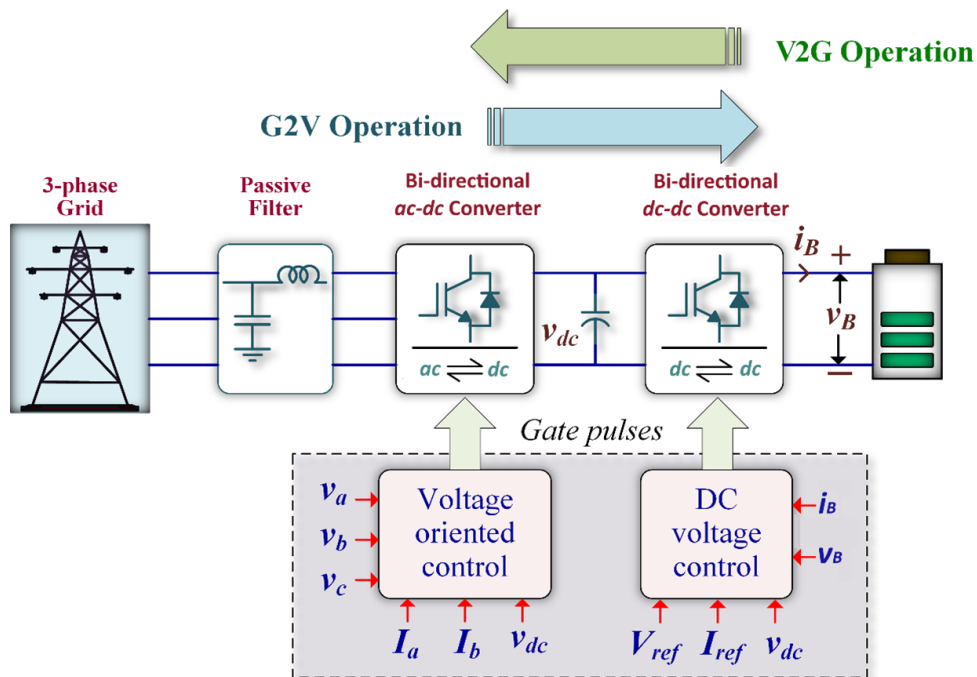


Figure 5. Overall block diagram of the vehicle-grid interface system.



The mode transition from V2G to G2V and vice-versa is an intricate process requiring various parameters on the grid and battery side to be monitored. The parameters at the grid side include phase sequence, frequency and magnitude of line voltages. At the battery side, the parameters like battery voltage, battery current, temperature and most importantly the battery state-of-charge [12, 15, 19, 20]. The order of power deemed fit for extraction from the battery or for it to be supplied to charge the battery is a function of battery state-of-charge. A suitable control strategy is employed at the PWM inverter as well as at the bi-directional  $dc - dc$  converter end for enabling the power structure to facilitate the desired bi-directional power flow between EV and the three-phase grid. The constituent parts or blocks contributing in achieving the desired bi-directional power flow is mentioned in the sections to follow. The overall block diagram representation of the vehicle-grid interface system is shown in Figure 5.

### 3. Vehicle-Grid interface building blocks

The first component that plays the role of being able to regulate, modulate, and control bi-directional power flow between the vehicle and the electrical grid is the PWM inverter. The PWM inverter chosen in this case is a conventional three-phase inverter with two power electronic switches (preferably IGBT) on each leg to be able to seamlessly transfer the power from grid to vehicle and vehicle to grid. The overall power structure of the PWM inverter with a bi-directional  $dc - dc$  converter is shown in Figure 6. The structure of the inverter remains the same in both the desired modes of operation i.e. V2G and G2V, with only the control signals or gating signals given to the power electronic switches altered to be able to control the power flow in either direction. Irrespective of the direction of power flow, synchronization with the electrical grid is necessary. To be able to synchronize the PWM inverter operation with the grid parameters, the grid voltages are always measured. This measurement apart from giving information about the magnitude of grid voltage, also gives information on the phase sequence as well as frequency of the grid. This enables the PWM inverter to act as a rectifier during the G2V mode and as an inverter during V2G mode.

The objective to transfer the power between EV battery and electrical grid depends on the control strategy being adopted to control the PWM inverter and  $dc - dc$  converter. In this work, voltage control oriented (VOC) is employed for controlling the output of PWM inverter in the rectifier as well as in inverter mode for G2V and V2G modes respectively. The control strategy aims to maintain the  $dc$  link voltage at the PWM inverter terminals to remain constant to a defined extent. The methodology adopted includes

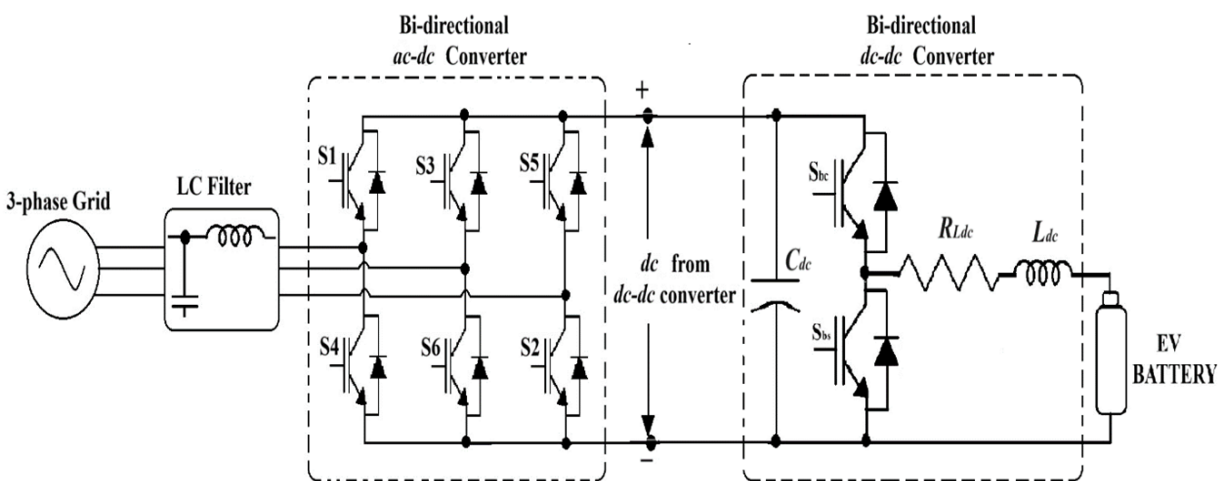
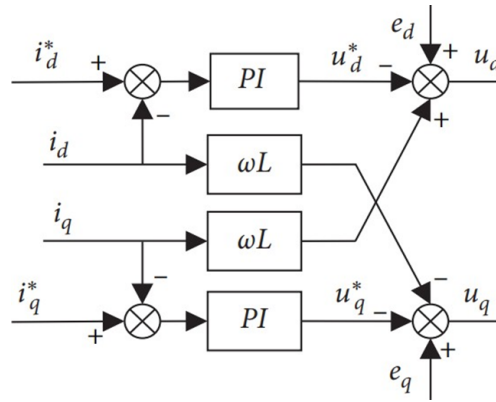


Figure 6. Power topology of bi-directional  $ac - dc$  and  $dc - dc$  converter.



**Figure 7.** Feed-forward based decoupling scheme.

measuring the ac voltages and currents from the grid side and transforming them from abc reference frame to d-q reference frame for being able to control the active and reactive power demand of the system.

The control loop consists of an outer-loop for based on voltage and an inner-loop based on current with individual PI (Proportional-Integral) controllers for improving the transient response of the system. In addition to it, a grid-voltage-based feed-forward decoupling scheme is also employed for enhancing the power transfer capability. Here,  $u_d^*$  and  $u_q^*$  are computed  $d - q$  axis voltages,  $e_d$  and  $e_q$  are reference  $d - q$  axis voltages,  $i_d^*$  and  $i_q^*$  are the reference currents. The modality used in the implementation of control scheme is to alter the values of  $i_d^*$  and  $i_q^*$  to control the active and reactive power transferring capability of the converter while interfaced with the grid. During the V2G mode this control scheme ensures that the active power injected into the electrical grid from the EV battery is modulated by keeping the dc link voltage at the inverter side constant. At the same time during the G2V mode, the PWM rectifier needs to convert the ac grid voltage into dc for it to be supplied to the  $dc - dc$  converter stage for charging the EV battery. Based on the state-of-charge of the battery, the value of dc voltage and dc current flowing into the battery needs to be altered which is controlled by the PWM rectifier. As the grid integration norms mandates that the harmonics in the current as well as the phase difference between current and respective voltage should be minimum, the control strategy adopted ensures that the current drawn from the grid is in-phase with the input voltage and it is maintaining unity power factor at the line side by also keeping the harmonics in the current under check as per the globally accepted power quality norms. For meeting the said requirement, the values of quadrature axis reference current is altered and preferably kept at zero for ensuring the harmonic level in the grid current is minimum (well under the stipulated limits) as well operate the converter at unity power factor. The control strategy with feed-forward based decoupling is shown in Figure 7.

Transformation from abc to  $\alpha - \beta$  axis and subsequent transformation from  $\alpha - \beta$  to  $d - q$  axis is an integral part of the adopted control scheme as it eliminates the dependence of the frequency component in the implementation system thereby making the adopted control system faster and more efficient. The transformation involving abc to  $\alpha - \beta$  and subsequently to  $d - q$  reference frame is enabled by carrying out the calculations as mentioned in equations (1) and (2),

$$\begin{bmatrix} V_\alpha(t) \\ V_\beta(t) \end{bmatrix} = \begin{bmatrix} \frac{2}{3} & \frac{-1}{3} & \frac{-1}{3} \\ 0 & \frac{1}{\sqrt{3}} & \frac{-1}{\sqrt{3}} \end{bmatrix} \begin{bmatrix} V_a(t) \\ V_b(t) \\ V_c(t) \end{bmatrix}, \quad (1)$$



$$\begin{bmatrix} V_d(t) \\ V_q(t) \end{bmatrix} = \begin{bmatrix} \cos(\theta(t)) & \sin(\theta(t)) \\ -\sin(\theta(t)) & \cos(\theta(t)) \end{bmatrix} \begin{bmatrix} V_\alpha(t) \\ V_\beta(t) \end{bmatrix}, \quad (2)$$

where  $V$  denoted the voltage or current quantity to be computed.  $V_\alpha$  and  $V_\beta$  are the stationary  $\alpha\beta$  frame quantities and  $V_d$  and  $V_q$  are the synchronous  $d - q$  frame quantities. The synchronization or phase locking of this system is realized by controlling the q-axis voltage to zero [7, 8]. Realizing the bi-directional flow of power from the three-phase converter to battery and vice-versa, the intermediate stage of  $dc - dc$  conversion between battery and three phase power converter is of utmost importance. The power topology of the said  $dc - dc$  converter is shown in Figure 6. Based on the mode of operation selected, whether V2G or G2V, the said  $dc - dc$  converter can perform Boost operation or Buck operation by turning on switching  $S_{bs}$  and  $S_{bc}$  respectively.

The control signals governing the working of  $dc - dc$  converter as a buck converter or boost converter in G2V and V2G mode respectively depends on the voltage reference  $V_{ref}$  and current reference  $I_{ref}$  to be obtained on the grid terminals at the point of common coupling as well as the battery voltage  $V_B$ , battery current  $I_B$  and the dc voltage at the PWM inverter terminals  $V_{dc}$ . Based on the values of the above-mentioned quantities, the proportional and integral (PI) controller generates control signal which when compared with the triangular pulses having frequency equal to switching frequency generates gating pulses which is then given to the switches  $S_{bc}$  and  $S_{bs}$  to decide the buck or boost operation of the  $dc - dc$  stage. The control scheme governing the buck or boost mode of operation is indicated in Figure 8 and Figure 9 respectively.

While employing the buck mode or boost mode, either constant voltage or constant current strategy respectively is employed with a dedicated PI controller to ensure the bi-directional power flow through  $dc - dc$  converter based in the demand raised by the user [13].

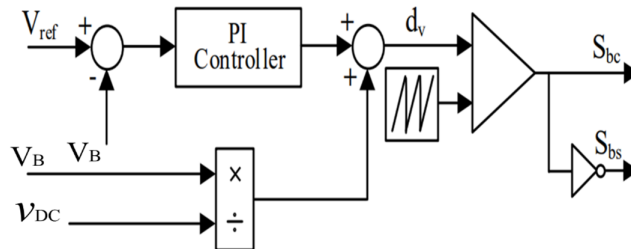


Figure 8. Control loop for buck operation.

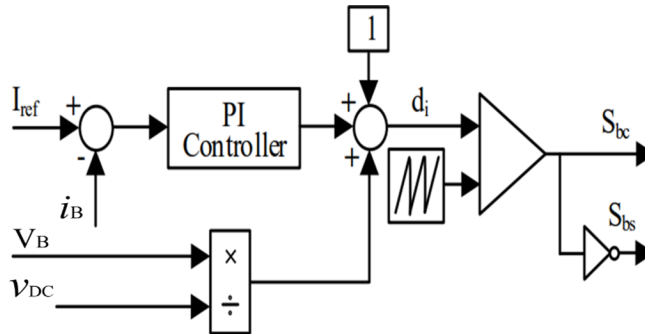
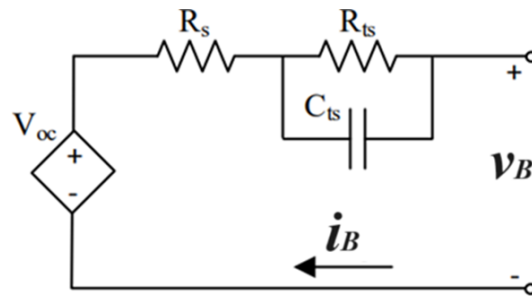


Figure 9. Control loop for boost operation.



**Figure 10.** Thevenin equivalent circuit of Li-ion battery, with  $V_{oc}$  as the open circuit battery voltage,  $R_s$  as the equivalent series resistance of the battery,  $R_{ts}$  and  $C_{ts}$  as the charge transfer phenomenon based on parallel resistance and capacitance, respectively,  $I_B$  as the battery current, and  $V_B$  as the battery terminal voltage.

The PI controller in the given control scheme for  $ac - dc$  and  $dc - dc$  converters is controlled using the controller output  $u(t)$  which is fed into the system to manipulate the variable input which in this case is the sensed quantities. The relationship of controller output  $u(t)$  can be given by equation (3),

$$u(t) = u_{bias} + K_c e(t) + \frac{K_c}{\tau_i} \int_0^t e(t) dt , \quad (3)$$

here,  $u_{bias}$  is constant that sets the value of  $u(t)$  when the controller is operated for the first time with initial values.  $K_c$  is the controller gain,  $\tau_i$  is the integral time constant and  $e(t)$  is the error set point.

The mathematical model of the battery also plays an important role in deciding the flow of power in the adopted vehicle-grid interface system. The mathematical model is incorporated in simulation and validation analysis to predict the variation of state of charge of the battery with load variation in an effective manner. On the same lines, the charge estimation while charging is employed and a suitable mode viz. constant voltage or constant current mode is accordingly selected [15]. The detailed model here equips the battery to be able to assess the state-of-charge using the conventional terminal voltage method, such that it is able to decide the change-over from V2G to G2V mode based on the input received from the user [9–11]. The battery model can be expressed using an equivalent Thevenin model as shown in Figure 10 [15].

## 4. Design calculations

### 4.1. LC filter design

The power structure is responsible for the seamless transfer of power from vehicle to grid and vice versa. Inverter has a significant role in this power structure. In the V2G mode, when the power is being transferred from EV battery to the grid through the inverter, the output voltage of the inverter will be having presence of high-frequency components synonymous with the switching frequency of the inverter. As per the grid compatibility norms, the said output of the inverter cannot be directly fed to the grid till the higher-order frequency terms are not filtered by using a passive filter. In the designed system, an LC filter is employed. The LC filter attenuates the higher frequency components and thereby prevents them from adversely impacting the grid operation. However, it is designed to pass the power frequency components without any attenuation. For the inverter, this facilitates it to be connected to the grid for active power injection during the V2G mode. For G2V mode, it acts to prevent the higher frequency components produced due to the operation of PWM rectifier for charging the EV battery from entering into the grid. In this process the power quality at the grid side is maintained as per the standards. The arrangement of

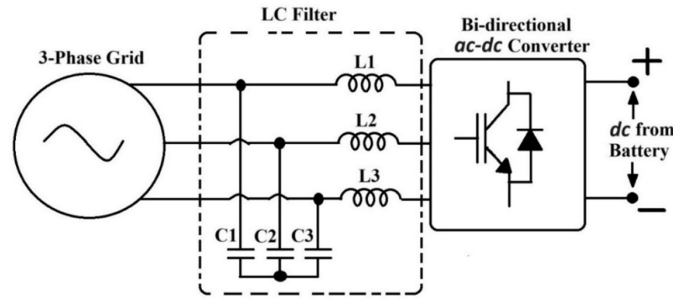


**Figure 11.** Arrangement of LC Filter with PWM Inverter.

LC filter at the output of the power converter is shown in Figure 11, where  $L_1, L_2, L_3$  are the line side inductances whereas  $C_1, C_2, C_3$  are the line side filter capacitances. The line side inductances are identical and are termed as  $L$ . The line side capacitances are also identical and are commonly termed as  $C$ .

While designing the values of inductance and capacitance in the LC filter, the estimation of the cut-off frequency,  $f_c$ , of the filter plays an important role. As per the IEEE standards,  $f_c$  is expressed as a function of switching frequency of the inverter,  $f_{sw}$ , using the following mathematical relationship is mathematically expressed as,

$$f_c < \frac{f_{sw}}{15} . \quad (4)$$

It is considered that the value of inductance considered in the LC filter accounts for 3% voltage drop with respect rms value of the fundamental line-line voltage of the inverter. Based on this, the maximum permissible inductor current,  $I_{Lmax}$ , is mathematically expressed in (5),

$$I_{Lmax} = \frac{0.03 \times V_{Lrms}}{2\pi \times f_c \times L} , \quad (5)$$

where  $V_{Lrms}$  is the fundamental rms line voltage at inverter output,  $f_c$  is the fundamental frequency of the voltage which is also the cut-off frequency at which the filter is tuned and  $L$  is the line inductance connected in the LC filter. Considering the values all the known parameters and substituting in equation (4), the value of  $L$  is calculated as 5 mH and the same has been used in the simulation and HIL based implementation. Similarly, the value of line capacitance  $C$  required to be connected in the LC filter can be found out from the equation (6),

$$C = \frac{1}{4\pi^2 \times f_c^2 \times L} . \quad (6)$$

#### 4.2. Switching inductor and capacitor design

The  $dc - dc$  converter which is utilized for bi-directional power flow from the EV battery and the grid requires inductor and capacitor at the output of the converter for maintaining the dc current and dc voltage being dumped into or drawn from the EV battery. The selection of the inductor and capacitor is based on the values of current ripple and voltage ripple allowed in the system. The value of switching inductor ( $L_{dc}$ ) and capacitor ( $C_{dc}$ ) connected with the  $dc - dc$  converter stage is calculated based on the ratings selected and specifications desired using the equations (7) and (8) respectively.

$$L_{dc} = \frac{V_{dc} \times (V_B - V_{dc})}{3 \times f_{sw} \times V_B} , \quad (7)$$

$$C_{dc} = \frac{I_{ripple}}{8 \times f_{sw} \times V_{ripple}} \quad (8)$$

where  $V_{dc}$  is the output dc link voltage at the inverter terminals and  $V_B$  is the input voltage at the terminals of the EV battery, ( $V_{ripple}$ ) and ( $I_{ripple}$ ) are voltage ripple and current ripple respectively.

## 5. HIL implementation steps

HIL is a rapid prototyping-based system which has a dedicated controller in the form of a Field Programmable Gate Array (FPGA) which helps in simulating and realizing the output of the circuit considering the conditions being encountered in the real-time scenario. The results of the said tool are considered comparable to actual hardware which in turn reduces the up-time for creating and testing an actual hardware [21]. The HIL system also has provisions to only run and execute the control strategy by integrating the power modules at the output / input ports of the HIL to create a hybrid execution system consisting of hardware integrated with software. In this study, OPAL-RT OP4510 is used for executing and validating the V2G and G2V system. The HIL system is integrated with actual hardware circuit comprising of the control cards, driver card as well as current and voltage sensors.

The inverter module is created as a project model in the RT lab software of OPAL-RT. The steps in HIL based plant model generation includes:

- **Circuit design stage:** A circuit/ model of the proposed system is created on the RT lab software in which at the back-end MATLAB/ Simulink is used. The block sets indicating the input ports, output ports as well as the feedback signals as well as their nature is decided and connected to the system accordingly.
- **Model compiling stage:** The model compiling stage follows the model creation stage. In this stage, the model is compiled and errors in the plant model are identified. Once the plant model compiling process is completed successfully, the plant model file in the exportable form becomes ready which can now be uploaded on the on-board FPGA controller for further execution.
- **Model flashing on embedded Target (FPGA Programming):** The executable compiled plant model file post successful compilation is now loaded on the on-board controller (FPGA). The real time simulator OPAL-RT once successful in loading the executable file is now ready for hardware implementation and real time execution.
- **Model implementation and execution:** The HIL implantation starts with this stage. The output and input ports configured for model execution exhibit the signals at the desired level as per the specified limits. The model starts fetching the feedback signals on the input ports based on the nature of signals (digital / analog) and as per the control strategy give the control signals to the power circuit through the output ports to complete the hardware implementation.

The stages involved in model execution using HIL as discussed in the above section are indicated in Figure 12. The stages are suggestive and gives an overall idea in the creation, configuration, compilation, loading as well as execution of the plant model in the real-time scenario as specified by the user.

## 6. Simulation and HIL implementation

An 18-kW power rating vehicle grid interface circuit is developed in MATLAB/Simulink and HIL using the above-mentioned block-sets. The control schemes for the  $ac - dc$  and  $dc - dc$  converters as discussed in the previous sections. The functional block diagram for the simulation study is shown in Figure 13. For the simulation study as well as for the HIL implementation, the battery parameters as well as the converter input and output ratings are of utmost importance. System parameters and Li-ion battery parameters are

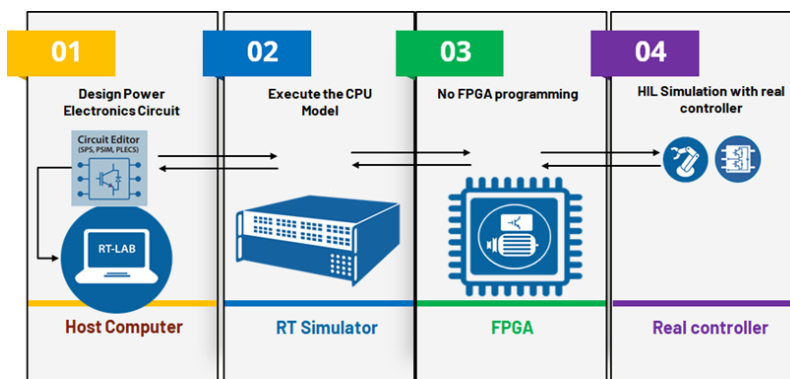


Figure 12. Stages of plant model execution on HIL.

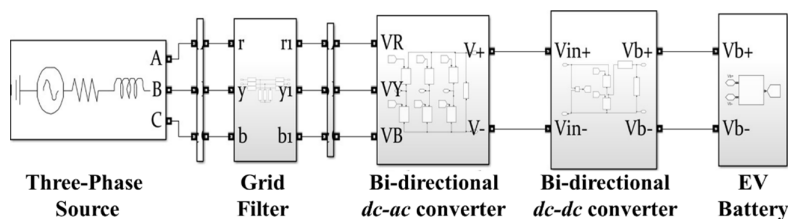


Figure 13. Simplified MATLAB Simulation Model of Bi-directional Converter.

shown in Table 1 and Table 2 respectively. The battery rating considered for simulation and HIL based implementation is of a low performance EV passenger vehicle or car having a 400 V dc-bus architecture. Since the EV considered in implementation of the V2G and G2V system is a low performance vehicle, it is indicative that the torque requirement and acceleration demanded from the vehicle is limited. This reflects on the current supported as well as charge capacity of the battery used.

The adopted  $ac - dc / dc - ac$  converter (bi-directional PWM inverter) is operated using the voltage-oriented control method. By virtue of the said method, the active power injected by the converter into the grid as well as the seamless changeover from V2G to G2V mode and vice versa is controlled. Similarly, in the case of  $dc - dc$  converter, battery state-of-charge estimation-based control scheme is used such that the battery charging and discharging could be done in well-defined and effective manner. The change-over between the G2V and V2G modes is also dependent upon the magnitude and polarity of battery current as indicated in the control block diagram discussed in the previous section. The battery current polarity is changed, based on which the control strategy takes the decision to operate the power scheme in either the V2G or G2V mode. The values of proportional gain ( $K_p$ ) and integral gain ( $K_i$ ) for all the converters operated in closed loop mode with V2G and G2V mode of operation is obtained and the said values are mentioned in Table 3.

Table 1. System Configuration.

Parameter	Value
Supply Line voltage $V_s$	415 V
Supply frequency $f_c$	50 Hz
Filter inductance $L$	5 mH
Filter Capacitance $C$	30 $\mu$ F
Switching frequency $f_{sw}$	10 kHz
DC link voltage $V_{dc}$	800 V

**Table 2.** Battery Parameters.

Parameter	Value
Nominal voltage $V_{bn}$	360 V
Fully charged voltage $V_{bf}$	419 V
Cut-off voltage $V_{bc}$	270 V
Initial state-of-charge $Q_0$	50%
Internal resistance $R_s$	0.07 $\Omega$
Rated capacity $Q$	50 Ah
Battery response time $T_r$	1 ms
Nominal discharge current $I_{bn}$	21.5 A

**Table 3.** PI Controller Values.

Converter	$ac - dc$ converter	$dc - dc$ converter
Proportional gain $K_p$	0.5	0.005
Integral gain $K_i$	5	10

## 7. Results and discussion

### 7.1. Simulation results

EV battery interfaced with grid through the cascade connection of  $dc - dc$  converter and an inverter along with the necessary control system is modelled in MATLAB/SIMULINK. The simulation parameters are as mentioned in Table 1 and 2. The simulation model is analyzed for: (a) G2V mode of operation, and (b) V2G mode of operation. During G2V mode, the bidirectional  $dc - dc$  converter is controlled to ensure that the battery voltage/current match the reference value as per the selected charging mode. This results in a drop in the dc-link voltage. In this mode, the inverter acts as a PWM rectifier to regulate the dc-link voltage and the commanded value. As the dc-link voltage is higher than the maximum voltage that can be withstood by the battery without sustaining the damage, the  $dc - dc$  converter needs to act as a step-down converter. Three phase grid voltages and current supplied by the grid are shown in Figure 14. The grid voltage is sinusoidal with the peak line-neutral voltage of 325V. The LC filter connected at the ac terminals of the inverter ensure that the switching harmonics are prevented from entering the grid. This is evident from absence of any distortions in the grid voltages. The currents supplied by the grid have the peak magnitude of 8.42A with %THD within the 5% limit.

From Figure 15 it is clear that the PWM rectifier operation results in the current and voltage for phase a being sinusoidal and in-phase, thereby indicating near unity power factor operation. Similar is the case for the other two phases. The harmonic spectrum for grid current during G2V mode is shown in Figure 16. As the current is in-phase with the respective line voltage and the current follows as sinusoidal envelope, the harmonic spectrum of line current is clean with the peak fundamental magnitude of 8.42 A, which is in adherence to the harmonic standards. This is due to the PWM rectifier being controlled to draw only the fundamental active current from the grid.

Figure 17 shows battery SoC, terminal voltage and current drawn by the battery during G2V mode. The battery SoC for initiating the charging process through G2V mode is fixed at 50%. In an endeavor to reduce losses and temperature, the charging current of the battery is set at 10 A which corresponds to 0.2 C-rating. The positive rate of change of SoC indicates that the battery is gradually charging. As the battery is being charged at 0.2 C-rate and the plot given in Figure 16 are over the 1s duration, the increase in terminal



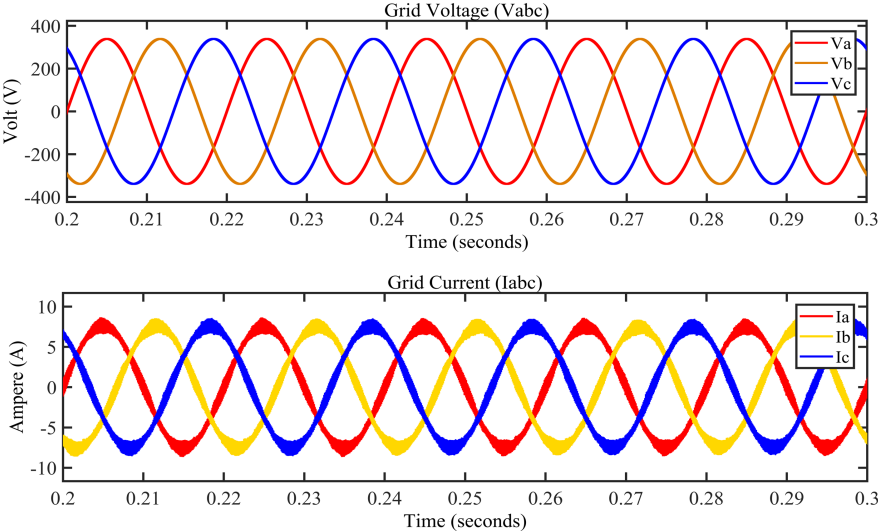


Figure 14. Grid Voltage ( $V_{abc}$ ) & Current ( $I_{abc}$ ) during G2V.

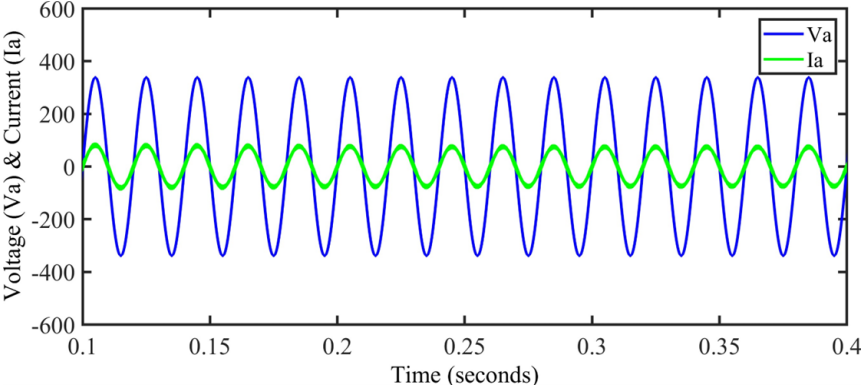


Figure 15. Voltage ( $V_a$ ) & Current ( $I_a$ ) during G2V.

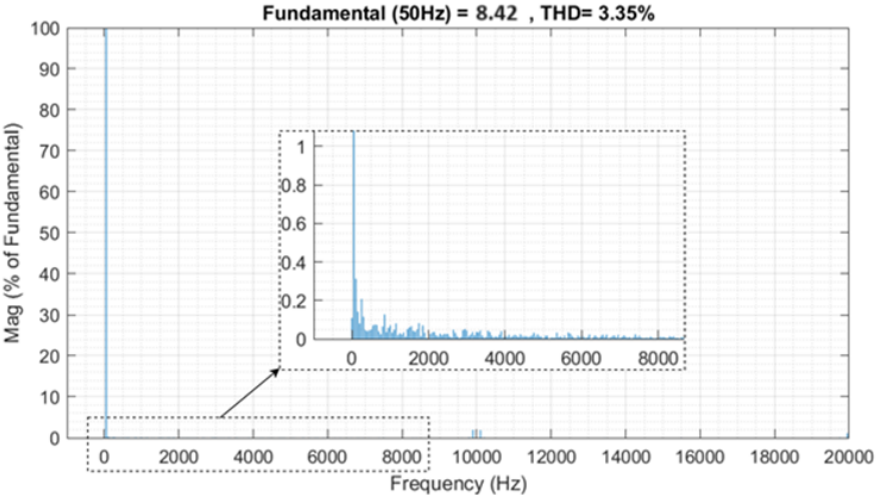
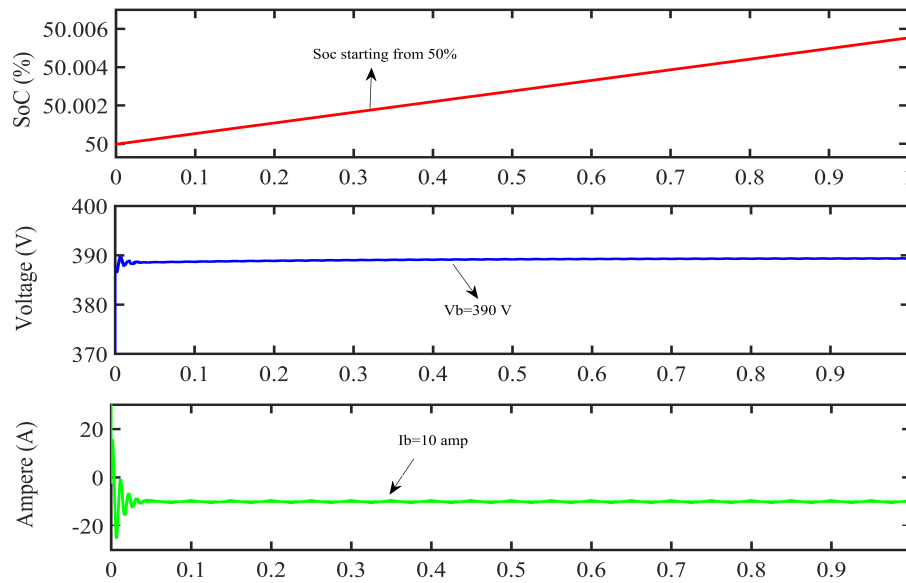


Figure 16. Harmonic Spectrum of the Input Line Current during G2V mode.



**Figure 17.** Battery SoC, Voltage ( $V_b$ ) & Current ( $I_b$ ) in G2V.

voltage is minimal. However, over longer time duration significant increase in terminal voltage would be experienced. The tuned value of PI controller used in the control scheme ensures that the magnitude of voltage across the battery is maintained constant at the same time the settling time of the circuit is fast enough. The figure also indicates that the ripple in dc-link voltage at the battery terminals is minimal (well within the assumed range). The control scheme with the PI controller also ensures that, the magnitude of EV battery current corresponding to rise in state of charge of the EV battery remains constant through out the charging cycle employed during G2V mode.

Conversely, during the implementation of V2G mode, the power flow starts from battery in the vehicle, and the power from this battery is injected into the grid using a PWM inverter. The stages involved between the vehicle battery and the grid are the bi-directional  $dc - dc$  converter as well as the bi-directional  $ac - dc$  converter (PWM inverter). The PWM inverter starts working as a grid-tied inverter.

During the V2G mode, it is desired to have a power flow from the electric vehicle to the grid. As per Figure 18, the bi-directional  $dc - dc$  converter acts as a boost converter which enhances the dc voltage of the battery from 388 V to around 800 V at the input of the PWM inverter. The battery's state-of-charge is continuously monitored, and it starts falling from the initial value of 50%, indicating that the discharging action of the EV battery has started. The current during the discharge condition is maintained at 10 A, which again corresponds to 0.2 C-rate of the battery. This C-rating is chosen to make sure that the losses and temperature rise associated with the battery is in a controlled manner. Figure 18 shows battery SoC, voltage and current waveform during G2V mode.

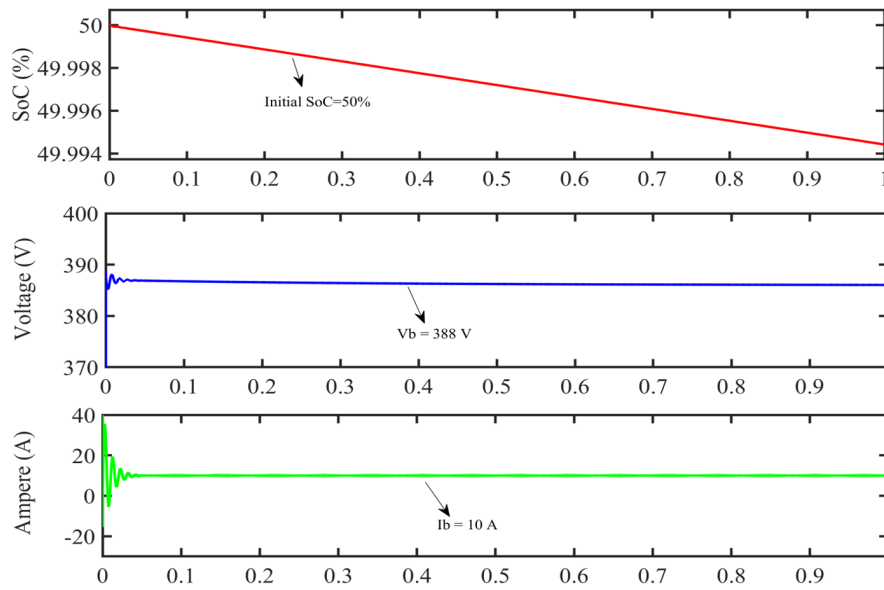


**Figure 18.** Battery SoC, Voltage ( $V_b$ ) & Current ( $I_b$ ) in V2G.

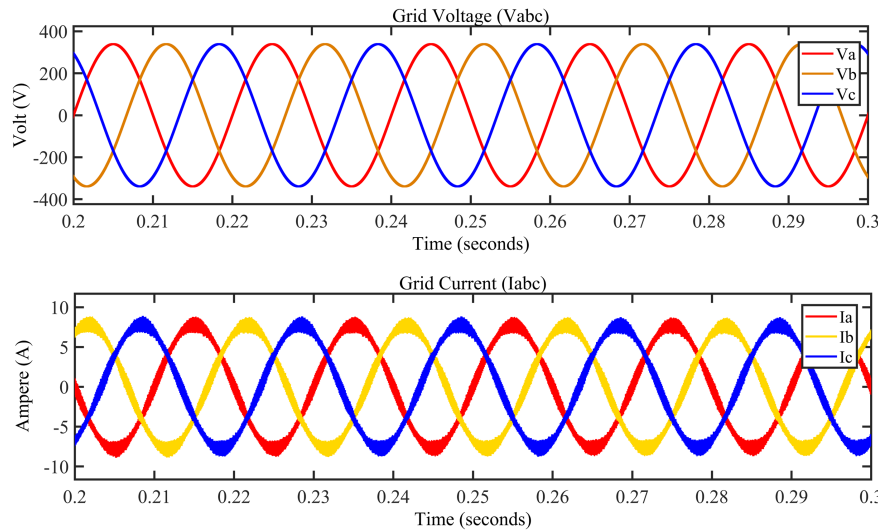


**Figure 19.** Grid Voltage ( $V_{abc}$ ) and Current ( $I_{abc}$ ) during V2G.

The results are indicative that the control scheme adopted for operating the converters in V2G mode are responding as per the desired way. The PI controllers are ensuring that the system remains stable by maintaining the dc link voltage at the  $dc - dc$  converter stage output such that the gradual discharge of the battery into the grid through PWM inverter can take place at constant C-rate. As shown in Figure 18, the line side or grid side phase voltages are obtained with a frequency of 50 Hz and a peak voltage of 315 V on each phase. As it is clear from the results, all the three-phase voltages are  $120^\circ$  phase shifted with respect to each other. Figure 19 also shows that the three-phase currents are  $120^\circ$  phase shifted with respect to each other. The amplitude of the current in all three phases is 8.35 A with a frequency of 50 Hz.

As the intended power flow is from vehicle to grid, the grid side phase voltage and grid side phase current injected by the vehicle into the grid will be out of phase with respect to each other. The nature of current injected into the grid at the point of common coupling is near to sinusoidal profile. The nature of

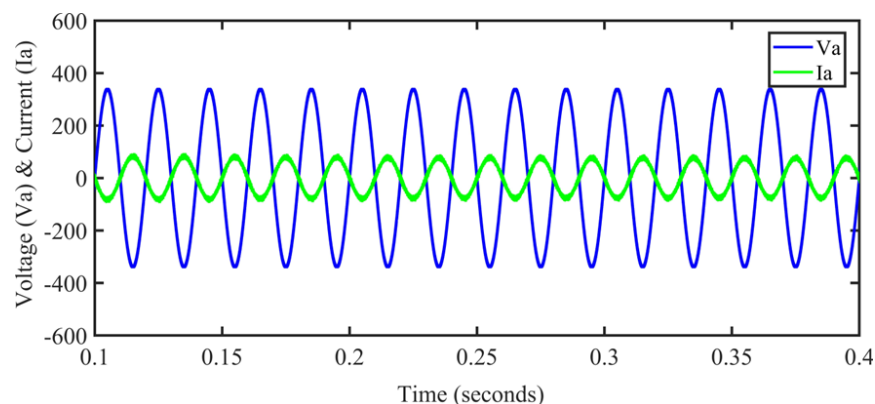


**Figure 20.** Voltage ( $V_a$ ) and Current ( $I_a$ ) during V2G.

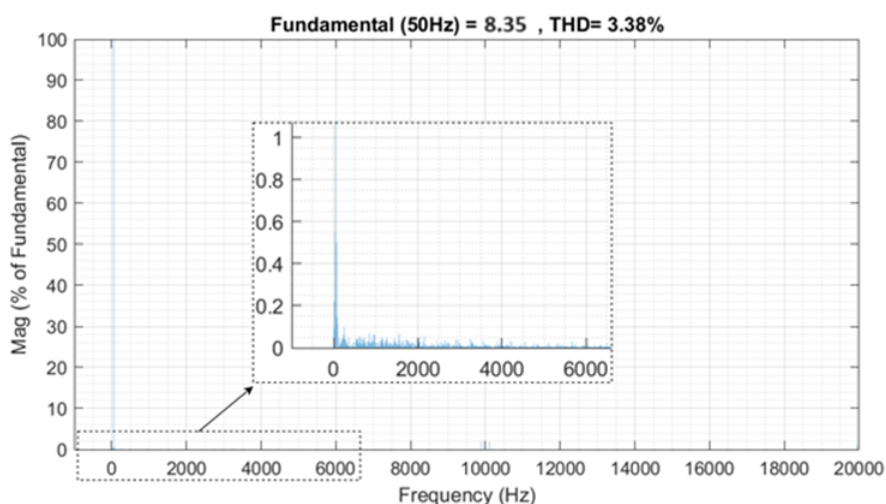


**Figure 21.** Harmonic Spectrum of the Input Line Current during G2V mode.

current injected into the grid at the output of PWM inverter is shown in Figure 20. The harmonic content in the current is well within the power quality prescribed limit and having a peak fundamental amplitude of 8.35 A. The harmonic content and harmonic spectrum of the grid side phase current is shown in Figure 21. The bi-directional  $dc - dc$  converter acts as a boost converter to supply higher dc link at the input of PWM inverter. The inverter starts injecting active power into the system by synchronizing the phase sequence, frequency and the magnitude of line voltage at the point of common coupling on the grid. The ac power injected by the PWM inverter passes through the passive LV filter which acts as a low pass filter and allows only fundamental frequency which is 50 Hz to enter into the grid and blocks the higher frequency components.

On the same lines, the combined operation of the vehicle-grid interface system is simulated, where the change-over from G2V to V2G mode is analyzed. The combined change-over or transition indicating G2V to V2G mode with its implication on the grid voltage and grid current is shown in Figure 22. The simulation results indicate a seamless transition of modes with the usage of the adopted control scheme in which the voltage-oriented control method looks after the bi-directional  $ac - dc$  converter and voltage-based control looks after the operation of bi-directional  $dc - dc$  converter. The results indicate that the variation in output line voltages at the grid side is minimal and the control scheme is able to maintain output voltage same as grid voltage. Also, mode change-over is indicated by the phase difference in the line current at the grid

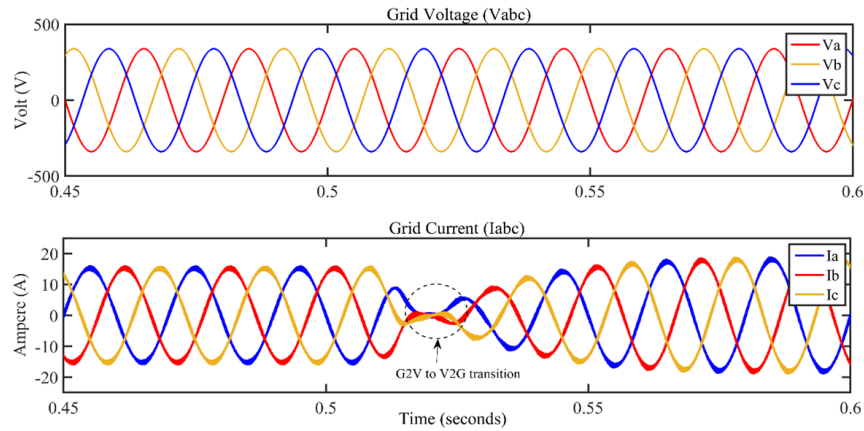


**Figure 22.** Grid voltage and grid current during G2V to V2G mode transition.

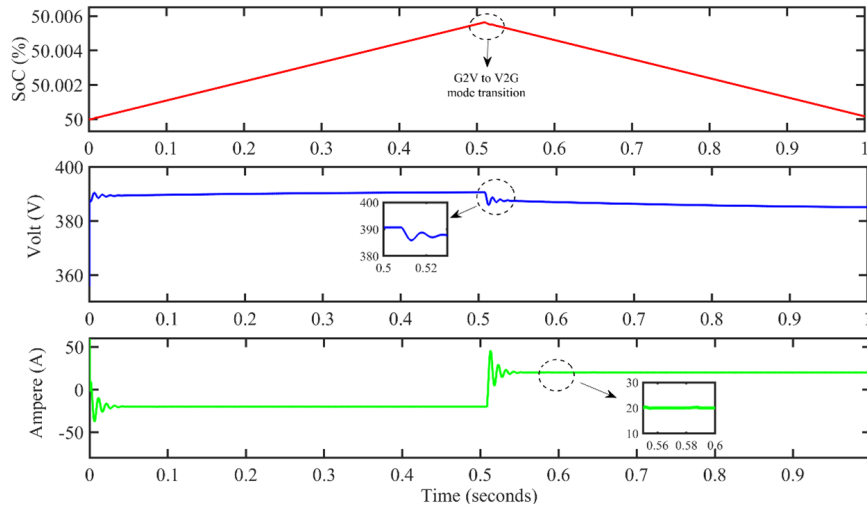


**Figure 23.** Battery SoC, battery voltage and battery current during G2V to V2G mode transition.

with respect to the grid voltage, where-in the current and voltage are in-phase during G2V mode and they become out of phase during V2G mode. The changeover from one mode to other as shown in Figure 22 is carried out within one cycle of the line to line grid voltage. The result also indicates that the settling time of the waveform during the mode transition is very low, which contemplates into effective tuning of the PI controller which is also integrated in the overall control block diagram of the proposed bi-directional power converter used for vehicle grid interface.

The impact on the battery voltage, battery state-of-charge and battery current is also analyzed for the mode transition. As can be seen in Figure 23, the battery state-of-charge increases till G2V mode is operational, the moment current reference of the battery is changed, the battery starts discharging leading to operation of the system in V2G mode. The line and load regulation capabilities of the bi-directional  $dc - dc$  converter is also validated by the fact that the battery voltage in both the modes of operation remains more-or-less constant with marginal variation which is taken care by PI controllers. Also, the battery current magnitude in both modes of operation is maintained at 10 A which is 0.2 C-rating of the battery. This again reflects that the PI controller action makes sure that the battery charging current and battery discharging current is maintained at constant level with gradual variation in battery state-of-charge during the G2V and V2G modes.

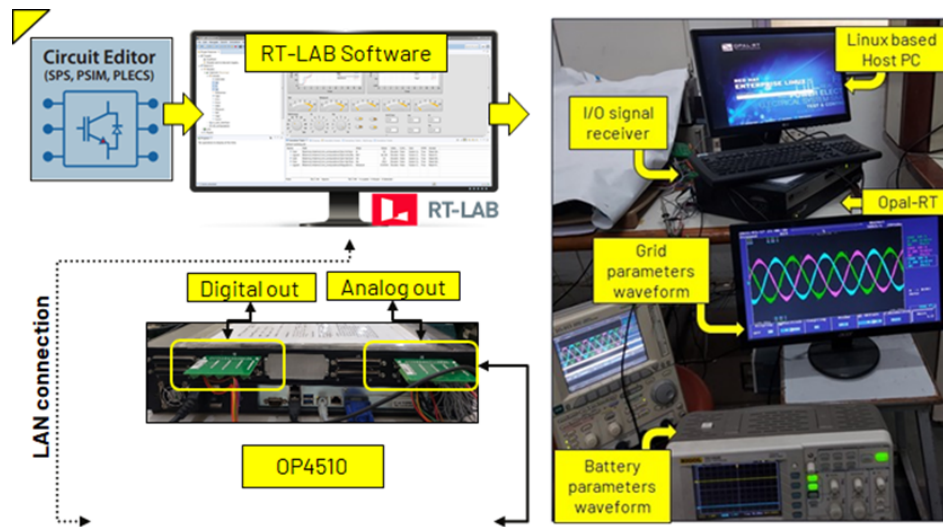


Figure 24. Hardware-In-Loop Setup.

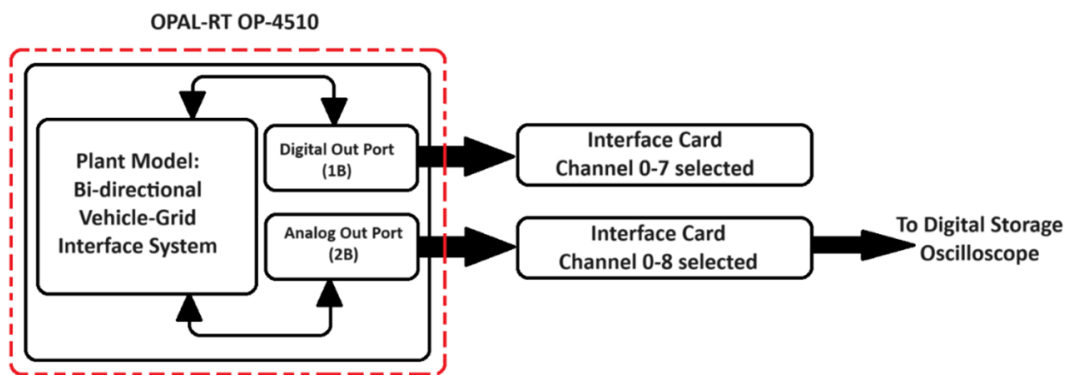


Figure 25. HIL Model Digital and Analog Port Configuration.

### 7.2. Hardware-In-Loop (HIL) results

During the HIL implementation, the plant model comprising of cascaded connection of grid connected PWM rectifier and bidirectional  $dc - dc$  converter is developed in the Real Time Simulator OPAL-RT using the MATLAB/SIMULINK interface. The HIL test setup is indicated in Figure 24. The system is equipped with input and output ports which take the real-time inputs and can give actual real-time outputs and reproduce the actual hardware output as per the plant model [12].

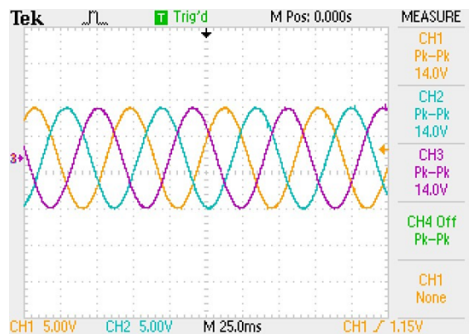
While exploring the functionality and implementation of HIL for the adopted control scheme, the analog and digital output ports of the HIL (OP-4510) are used. There are two ports, namely 1A and 1B for Digital IN / OUT. Similarly, ports 2A and 2B are used as Analog IN / OUT. In the presented work, ports 1B and 2B are configured as digital IN and analog OUT. The channels as per the requirement of the control loop as well as observation need on digital storage oscilloscope are selected, which is mentioned and shown in Figure 25.

Grid voltage and current waveforms are shown in Figure 26 (a) and (b). Signals are scaled down by factor 50 and 0.5 to match up with the output voltage limits of the ports on the HIL. From Figure 26 (c), in charging mode,  $V_q$  and  $I_a$  are at the same frequency and phase. On the contrary, in discharging mode,

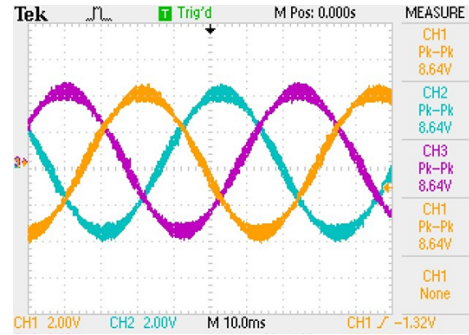


the current and voltage are at the same frequency but out of phase as per Figure 26 (d). From Figure 26 (e), before power flow reverses, the battery is discharging in the load, which means that the bidirectional AC/DC converter works under inverter state. After power flow reverses, the battery starts charging which represents converter working in rectifier mode. When the power flow changes, the voltage increased about 65 V and is restored to the original voltage level of 800 V after 210 ms.

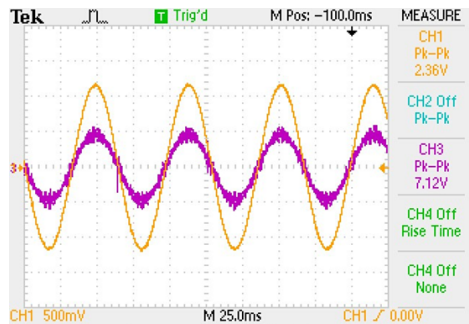
From the Figure 26 (f), initial battery current of 5 A flows and output current settles to new value of 10 A after 20 msec time duration. As a result, the converter is stable and works well in the power flow reversal condition. The HIL simulation results validates the designed control strategy in terms of system dynamics and it tracks or matches the results of simulation studies.



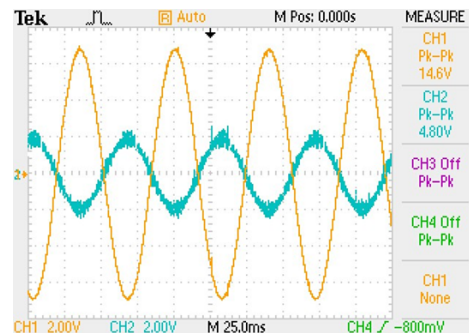
(a) Grid voltage.



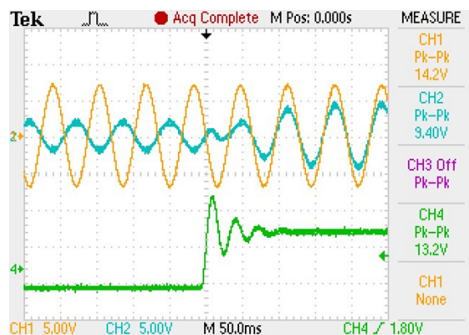
(b) Grid current.



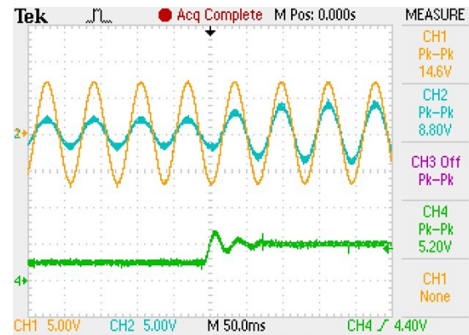
(c) Grid voltage and current during G2V mode.



(d) Grid voltage and current during V2G.



(e) Grid voltage and current from V2G to G2V.



(f) Grid voltage and current during load transition in G2V mode

**Figure 26.** HIL Validation Results using the Opal-RT 4510 simulator & RT-LAB software.

## 8. Conclusions

The topology and control algorithms of the battery charger proposed in this study are verified by Hardware-in-the-Loop (HIL) simulation utilizing the Opal-RT 4510 simulator and RT-LAB software. This research presents a model of an on-board bidirectional converter that facilitates two-way power flow interaction. This technology holds significant importance in the context of future smart grid scenarios. The control strategies for the battery-interfaced  $dc - dc$  converter and the grid-tied bidirectional  $ac - dc$  converter have been developed and implemented using Simulink. The HIL simulation results provide validation for the dynamic behavior of the built model. Based on the findings presented, it can be concluded that the bidirectional EV charging holds significant potential for utilizing electric vehicles as energy storage devices when they are accessible. Nevertheless, this notion presents numerous possibilities, necessitating additional investigation into the impacts of vehicle-to-grid (V2G) operating inside a localized distribution network. The study comprising of simulation and HIL based studies indicate that the bi-directional power flow between vehicle and grid is seamless and follows the control command of the user. The implementation methodology depicted in the study can serve as a reference model enabling implementation of various other bidirectional power flow converter models as per the requirement of the system. Also, the work carried out gives a clear idea about the aspects of rapid prototyping with an insight into the steps to be employed for implementing the bi-directional converter on the hardware-in-loop (HIL) system.

## Acknowledgments

The authors would like to thank Nirma University for providing the necessary hardware support in the form of hardware-in-loop system as well as the infrastructural facility for carrying out the necessary research work. This work is an outcome from the Minor Research Project grant for the project titled “Fabrication of Bi-directional Converter for Vehicle-Grid Interface” funded by Nirma University.

**Author contributions:** Each author made a substantial contribution to the conception and design of the research, experimental work, data analysis, and interpretation based on software and hardware results. All authors contributed equally to the drafting of this manuscript.

**Disclosure statement:** The authors declare no conflict of interest.

## References

- [1] Vítor Monteiro, J.G. Pinto, and João L. Afonso. Improved vehicle-for-grid (iv4g) mode: Novel operation mode for evs battery chargers in smart grids. *International Journal of Electrical Power & Energy Systems*, 110:579–587, September 2019.
- [2] Azhar Ul-Haq, Carlo Cecati, and Essam Al-Ammar. Modeling of a photovoltaic-powered electric vehicle charging station with vehicle-to-grid implementation. *Energies*, 10(1):4, December 2016.
- [3] Jiuchun Jiang, Yan Bao, and Le Wang. Topology of a bidirectional converter for energy interaction between electric vehicles and the grid. *Energies*, 7(8):4858–4894, July 2014.
- [4] Daouda Mande, João Pedro Trovão, and Minh Cao Ta. Comprehensive review on main topologies of impedance source inverter used in electric vehicle applications. *World Electric Vehicle Journal*, 11(2):37, April 2020.
- [5] Omar Ellabban, Joeri Van Mierlo, and Philippe Lataire. Control of a bidirectional z-source inverter for electric vehicle applications in different operation modes. *Journal of Power Electronics*, 11(2):120–131, March 2011.
- [6] R. Sivapriyan and S. Umashankar. Comparative analysis of pwm controlling techniques of single phase z-source inverter. *Indian Journal of Science and Technology*, 9(26), July 2016.

- [7] Zirui Jia and Liyuan Chen. Design of a bidirectional power interface for v2g technology with smaller dc-link capacitance. *International Journal of Smart Grid and Clean Energy*, 3(1):104–110, 2014.
- [8] Jingang Han, Xiong Zhou, Song Lu, and Pinxuan Zhao. A three-phase bidirectional grid-connected ac/dc converter for v2g applications. *Journal of Control Science and Engineering*, 2020:1–12, September 2020.
- [9] Vaibhav Shah and Saifullah Payami. Integrated converter with g2v, v2g, and dc/v2v charging capabilities for switched reluctance motor drive-train based ev application. *IEEE Transactions on Industry Applications*, 59(3):3837–3850, May 2023.
- [10] Shuo Liu, Xu Xie, and Liyong Yang. Analysis, modeling and implementation of a switching bi-directional buck-boost converter based on electric vehicle hybrid energy storage for v2g system. *IEEE Access*, 8:65868–65879, 2020.
- [11] Md. Mejbaul Haque, Peter Wolfs, Sanath Alahakoon, Bjorn C. P. Sturmberg, Mithulananthan Nadarajah, and Firuz Zare. Dab converter with q capability for bess/ev applications to allow v2h/v2g services. *IEEE Transactions on Industry Applications*, 58(1):468–480, January 2022.
- [12] Henri Josephson Raheerimihaja, Qianfan Zhang, Guoqiang Xu, and Xi Zhang. Integration of battery charging process for evs into segmented three-phase motor drive with v2g-mode capability. *IEEE Transactions on Industrial Electronics*, 68(4):2834–2844, April 2021.
- [13] P Pany, RK Singh, and RK Tripathi. Bidirectional dc-dc converter fed drive for electric vehicle system. *International Journal of Engineering, Science and Technology*, 3(3), July 2011.
- [14] Muhammad Harunur Rashid. *Power Electronics: Devices, Circuits, and Applications: International Edition*. Pearson, 2013.
- [15] Aziz Rachid, Hassan El Fadil, and Fouad Giri. Dual stage cc-cv charge method for controlling dc-dc power converter in bev charger. *2018 19th IEEE Mediterranean Electrotechnical Conference (MELECON)*, May 2018.
- [16] Ifiok Anthony Umoren, Muhammad Zeeshan Shakir, and Hina Tabassum. Resource efficient vehicle-to-grid (v2g) communication systems for electric vehicle enabled microgrids. *IEEE Transactions on Intelligent Transportation Systems*, 22(7):4171–4180, July 2021.
- [17] Rajendra Prasad Upputuri and Bidyadhar Subudhi. A comprehensive review and performance evaluation of bidirectional charger topologies for v2g/g2v operations in ev applications. *IEEE Transactions on Transportation Electrification*, 10(1):583–595, March 2024.
- [18] Saeed Golestan, Josep M. Guerrero, and Juan C. Vasquez. Three-phase plls: A review of recent advances. *IEEE Transactions on Power Electronics*, 32(3):1894–1907, March 2017.
- [19] Zheng Wang, Yue Zhang, Shuai You, Huafeng Xiao, and Ming Cheng. An integrated power conversion system for electric traction and v2g operation in electric vehicles with a small film capacitor. *IEEE Transactions on Power Electronics*, 35(5):5066–5077, May 2020.
- [20] Haris M. Khalid and Jimmy C.-H. Peng. Bidirectional charging in v2g systems: An in-cell variation analysis of vehicle batteries. *IEEE Systems Journal*, 14(3):3665–3675, September 2020.
- [21] José Aravena, Dante Carrasco, Matias Diaz, Matias Uriarte, Felix Rojas, Roberto Cardenas, and Juan Carlos Travieso. Design and implementation of a low-cost real-time control platform for power electronics applications. *Energies*, 13(6):1527, March 2020.